



# Suction based mechanical characterization of superficial facial soft tissues



J. Weickenmeier<sup>a,b</sup>, M. Jabareen<sup>c,\*</sup>, E. Mazza<sup>a,d</sup>

<sup>a</sup> Department of Mechanical and Process Engineering, ETH Zurich, Zurich, Switzerland

<sup>b</sup> Department of Mechanical Engineering, Stanford University, Stanford, USA

<sup>c</sup> Faculty of Civil and Environmental Engineering, Technion - Israel Institute of Technology, Haifa, Israel

<sup>d</sup> Swiss Federal Laboratories for Materials Science and Technology, EMPA Dübendorf, Dübendorf, Switzerland

## ARTICLE INFO

### Article history:

Accepted 25 October 2015

### Keywords:

Elasto-viscoplastic model

Facial skin and SMAS

Suction measurements

Inverse finite element analysis

## ABSTRACT

The present study is aimed at a combined experimental and numerical investigation of the mechanical response of superficial facial tissues. Suction based experiments provide the location, time, and history dependent behavior of skin and SMAS (superficial musculoaponeurotic system) by means of Cutometer and Aspiration measurements. The suction method is particularly suitable for in vivo, multi-axial testing of soft biological tissue including a high repeatability in subsequent tests. The campaign comprises three measurement sites in the face, i.e. jaw, parotid, and forehead, using two different loading profiles (instantaneous loading and a linearly increasing and decreasing loading curve), multiple loading magnitudes, and cyclic loading cases to quantify **history dependent behavior**. In an inverse finite element analysis based on anatomically detailed models an optimized set of material parameters for the implementation of an elastic-viscoplastic material model was determined, yielding an initial shear modulus of 2.32 kPa for skin and 0.05 kPa for SMAS, respectively. Apex displacements at maximum instantaneous and linear loading showed significant location specificity with variations of up to 18% with respect to the facial average response while observing variations in repeated measurements in the same location of less than 12%. In summary, the proposed parameter sets for skin and SMAS are shown to provide remarkable agreement between the experimentally observed and numerically predicted tissue response under all loading conditions considered in the present study, including cyclic tests.

© 2015 Elsevier Ltd. All rights reserved.

## 1. Introduction

There is increasing need for simulations of tissue behavior in facial expressions and medical applications, ranging from the planning of surgical procedures to the prediction of age related tissue changes. As a consequence, improved numerical modeling and reliable experimental characterization of the mechanical response of individual soft tissues are required.

The specific tissue composition including collagen, elastin, and the hydrated matrix of proteoglycans in facial soft tissues causes a highly nonlinear, pronounced anisotropic and heterogeneous response characterized by large deformations upon physiological loading, hysteresis, (nearly) incompressible, and often poroelastic tissue response (Fung, 1993). Several measurement techniques have been proposed to quantify the time and history dependent behavior of soft tissues, morphological changes over time as well as inherent transient behavior of the elastin and collagen fiber

network (Bischoff et al., 2004). Non-invasive testing methods include suction measurements (Hendriks et al., 2006; Iivarinen et al., 2014; Piérard et al., 2013a,b; Tarsi et al., 2013; Kauer et al., 2002; Nava et al., 2004; Hollenstein et al., 2013; Barbarino et al., 2011), indentation experiments (Abellan et al., 2013; Iivarinen et al., 2014), and in situ tension tests (Bhushan et al., 2010; Flynn et al., 2011; Jor et al., 2011). The experimental characterization of superficial facial tissue properties presented here is based on the suction method for its (i) simple applicability at each measurement site, (ii) non-invasiveness, (iii) in vivo suitability, (iv) capability to target a specific tissue layer by adapting the probe opening diameter, (v) multiaxial state of deformation closer to physiological loading cases (in contrast to uniaxial tension or torsion tests), and (vi) comparability of results with existing data (Barbarino et al., 2011; Weickenmeier and Jabareen, 2014).

Due to locally varying anatomical features in the face and forehead, the mechanical tissue properties in three different regions, i.e. jaw, parotid, and forehead, are related to the constituents of the location specific tissue structures. The jaw region is characterized by a soft tissue structure allowing increased deformability for speech and facial expressions. The forehead region has a densely connected

\* Corresponding author.

E-mail address: [cvmah@tx.technion.ac.il](mailto:cvmah@tx.technion.ac.il) (M. Jabareen).

<sup>1</sup> Neubauer Assistant Professor.

layered tissue structure including muscle fibers. Finally, the parotid region provides significant support to the tissues of the cheek due to the presence of the fibrous and stiff superficial musculoaponeurotic system (SMAS). The present study focuses on the two most superficial layers of the face, that is skin and SMAS. While skin consists of epidermis and dermis, the constituents of SMAS may vary by location as investigated by Ghassemi et al. (2003) who identified two different types of SMAS in the face.

The objectives of the present work are twofold. First, a suction based experimental procedure is developed for a reliable and repeatable mechanical characterization of the location, time, and history dependent behavior of superficial facial skin and SMAS. Second, the experimental data are used in a parameter optimization scheme to determine two specific parameter sets for the elastic-viscoplastic material model introduced by Rubin and Bodner (2002).

## 2. Experimental methods

### 2.1. Experimental setup

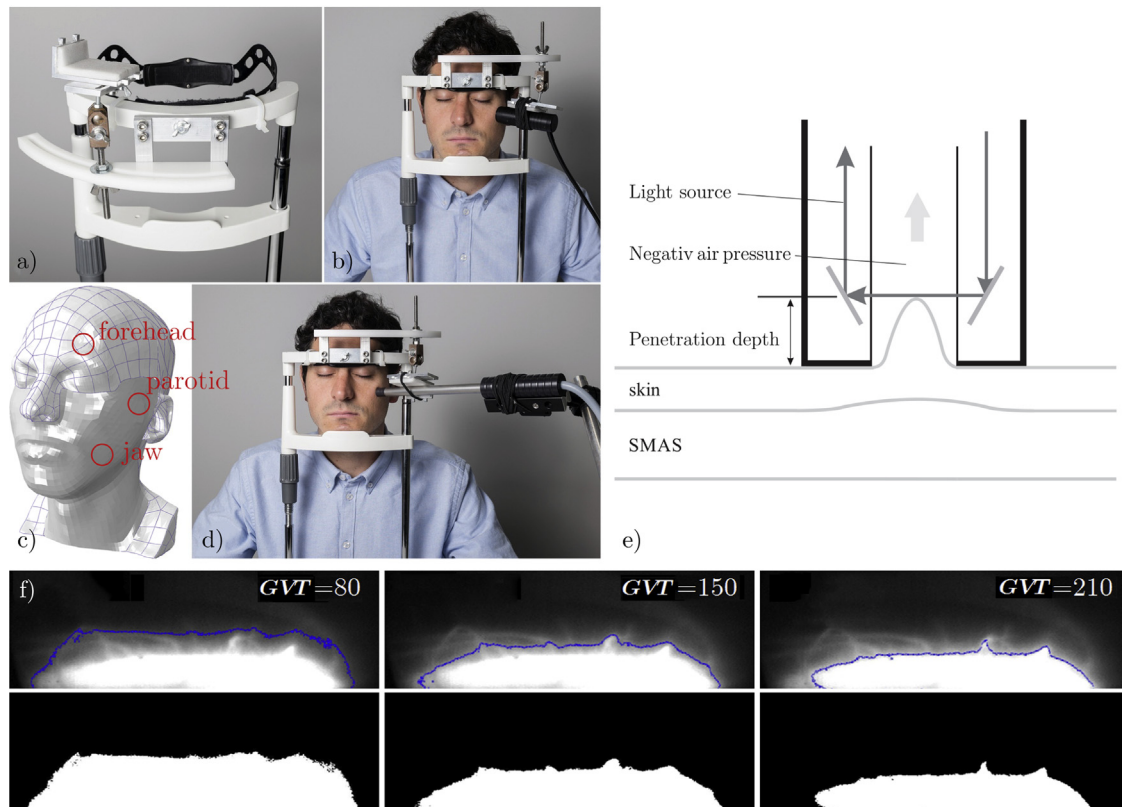
The present experimental campaign investigates the mechanical behavior of facial skin and SMAS by means of suction based measurements capturing the dependence of the mechanical tissue response with respect to (i) measurement location, (ii) transient response, and (iii) different loading profiles. The experimental setup, as shown in Fig. 1(a, b, d), is comprised of a headrest commonly used in ophthalmology which was modified such as to include a clamping tool for the probehead of both suction devices. A rigid fixation of the subject's head minimizes inherent sources of error in suction experiments by providing (i) optimal and repeatable probe placement with respect to specific measurement sites, (ii) reliable control of contact pressures, and (iii) minimal disturbance from relative movements between skin surface and probehead during individual measurements. Two different suction devices were used: the commercially available Cutometer MPA580 (Courage and Khazaka, 2014) with an opening diameter of 2 mm to address the

most superficial layer skin and the Aspiration device with an opening diameter of 8 mm to involve both, skin and the underlying layer of SMAS.

For both devices, the measurement principle is based on generating a negative pressure inside the probe cavity causing tissue to be sucked in, as shown schematically in Fig. 1(e). An optical system captures the deformation profile of the tissue during the entire loading cycle. In case of the Cutometer, a light sensor is used to correlate light intensity with tissue deformation in form of the apex height relative to the initial deformation prior to the measurement. In case of the Aspiration device developed at ETH Zurich (Kauer et al., 2002; Nava et al., 2004; Hollenstein et al., 2013), the optical system provides the 2D profile of the tissue bubble in form of an image sequence. Through subsequent image processing the initial tissue height and the evolution of apex displacement are extracted. This analysis is based on an image conversion from *gray-scale* to *black-and-white* images by means of a gray-value threshold (GVT). This allows us to differentiate between the deformed tissue and the background as shown for three distinct threshold values in Fig. 1(f). The GVT is determined manually by visual judgment of sample images to identify an appropriate value which may vary for different measurement sites as it strongly depends on skin type, surface shape, and lighting settings.

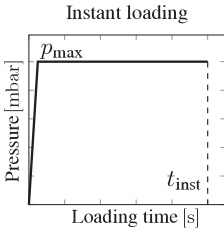
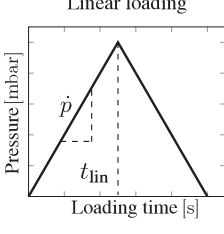
### 2.2. Measurement protocols

In order to activate the mechanical tissue properties related to varying time scales two different loading profiles were defined: instant and linear loading. *Instant loading* refers to measurements of instantaneous loading of the tissue to the full negative load ( $p_{max}$ ) which is held constant for the time span denoted by  $t_{inst}$ . The small retardation time during the loading phase up to  $p_{max}$  is predetermined by the individual controllers of the two devices. Instantaneous loading reveals the (short term) elastic as well as the long term tissue response. *Linear loading* refers to the linearly increasing and decreasing loading at a constant pressure rate. This loading mode activates deformation mechanisms with intermediate time scales which include fluid flow through porous layers. Table 1 summarizes all loading profiles which follow previous work (Barbarino et al., 2011; Weickenmeier and Jabareen, 2014). Varying loading magnitudes provide additional quantification of the tissues nonlinear deformation behavior. Each loading case is repeated at least four times to quantify variations in tissue response where waiting times of 45 s between individual measurements are enforced in order to allow for the tissues to recover. Additional measurements with shorter waiting times between repeated measurements revealed a memory effect on the soft tissue response while longer waiting times



**Fig. 1.** Experimental setup for the characterization of skin and SMAS. The measurement system contains a modified headrest (a) for high flexibility of the positioning and alignment of the (b) Cutometer and (d) Aspiration suction probes. To quantify location specific material behavior three different measurement sites are tested (c). (e) Schematic representation of the suction measurement principle. (f) Sensitivity analysis on one Aspiration image with three different GVTs to show its impact on skin tissue contour detection.

**Table 1**  
Loading protocols defined for the Cutometer and Aspiration measurements.

	Cutometer	Aspiration
 <p>Instant loading</p>	$p_{\max} = 300\text{mbar}$ $t_{\text{inst}} = 60\text{s}$  $p_{\max} = 500\text{mbar}$ $t_{\text{inst}} = 60\text{s}$	$p_{\max} = 66\text{mbar}$ $t_{\text{inst}} = 31\text{s}$  $p_{\max} = 133\text{mbar}$ $t_{\text{inst}} = 31\text{s}$  $p_{\max} = 200\text{mbar}$ $t_{\text{inst}} = 31\text{s}$
 <p>Linear loading</p>	$\dot{p} = 10\text{mbar/s}$ $t_{\text{lin}} = 17.5\text{s}$  $\dot{p} = 15\text{mbar/s}$ $t_{\text{lin}} = 17.5\text{s}$  $\dot{p} = 20\text{mbar/s}$ $t_{\text{lin}} = 17.5\text{s}$	$\dot{p} = 15\text{mbar/s}$ $t_{\text{lin}} = 10\text{s}$  $\dot{p} = 20\text{mbar/s}$ $t_{\text{lin}} = 10\text{s}$  $\dot{p} = 30\text{mbar/s}$ $t_{\text{lin}} = 10\text{s}$

showed neither a significant change in the tissues reference state nor a history dependent tissue behavior. The latter was specifically analyzed in cyclic tests considering four selective loading profiles (Cutometer: instant 300 mbar, linear 20 mbar/s and Aspiration: instant 200 mbar, linear 20 mbar/s). These measurements consist of three repetitions of the individual loading case with an intermediate unloading phase of 3 s. In total more than 150 Cutometer and Aspiration measurements on the same 29 year old male subject were performed, thus providing an elaborate quantification of the mechanical behavior of skin and SMAS.

### 3. Modeling

#### 3.1. Rubin and Bodner material model

The strain energy function ( $W$ ) proposed by Rubin and Bodner (2002) is particularly suitable for facial soft tissues and considers these as composite-like materials composed of an elastic material, elastic fibers, and a dissipative elastic-viscoplastic component. The specific form of  $W$  is given by

$$W = \frac{\mu_0}{2q}(e^{qg} - 1), \quad (1)$$

where  $\mu_0$  and  $q$  are material parameters, and the function  $g = \widehat{g}(J, \beta_1, \lambda_I, \alpha_1)$  was decoupled into four parts such that

$$\begin{aligned} \widehat{g}(J, \beta_1, \lambda_I, \alpha_1) &= \widehat{g}_1(J) + \widehat{g}_2(\beta_1) + \widehat{g}_3(\lambda_I) + \widehat{g}_4(\alpha_1), \\ \widehat{g}_1(J) &= 2m_1(J - 1 - \ln(J)), \widehat{g}_2(\beta_1) = m_2(\beta_1 - 3), \\ \widehat{g}_3(\lambda_I) &= \frac{m_3}{m_4} \sum_{i=1}^{N_{\text{fb}}} (\lambda_i - 1)^{2m_4}, \widehat{g}_4(\alpha_1) = m_5(\alpha_1 - 3), \end{aligned} \quad (2)$$

where  $\{m_1, \dots, m_5\}$  are additional material parameters. The individual parts of  $g$  include the function  $\widehat{g}_1(J)$  accounting for total volume dilatation,  $\widehat{g}_2(\beta_1)$  accounting for the distortional deformation of the isotropic matrix,  $\widehat{g}_3(\lambda_I)$  accounting for the fiber stretch, and  $\widehat{g}_4(\alpha_1)$  accounting for the elastic distortional deformation of the dissipative component of the model. In (2d),  $\langle \bullet \rangle = (|\bullet| + \bullet)/2$  are the McAuley brackets that eliminate the energy contribution of fiber families under compression. The strain energy function is defined in terms of the invariants of the total elastic distortional deformation,  $\mathbf{b}'$ , and the elastic distortional deformation of the dissipative component,  $\mathbf{b}'_{de}$ . The deformation measures and the hardening variable are governed

by evolution equations including a formulation for the magnitude of the rate of inelasticity and the hardening measure. In previously published work (Weickenmeier and Jabareen, 2014), the full Rubin and Bodner model was implemented within the finite element (FE) environment based on a mixed FE formulation. The proposed numerical scheme includes the introduction of the *relative deformation gradient* which maps the deformation between the current and the last converged step, as well as a strongly objective integration scheme particularly suitable for the evolution equations of elastic-viscoplastic material models. For a more detailed description of the concise derivation and implementation of the numerical scheme the reader is referred to Weickenmeier and Jabareen (2014).

#### 3.2. FE modeling of the suction experiments

The present simulations are based on two FE models derived from medical images of facial skin using high resolution ultrasonography. Layer thicknesses of superficial tissues relevant for the finite element models shown in Fig. 2, were measured using a General Electric NEW LOGIQ E9 machine with a linear array 18 MHz hockey stick probehead (L8-18i). The Cutometer model is a two-layered structure with layer thicknesses of 1.7 mm for skin and 3.0 mm for SMAS and a radius of 25 mm. The Aspiration model is a three-layered model including skin (1.7 mm) and SMAS (3.0 mm), a third layer of muscle (5 mm), and a radius of 72.5 mm. The third layer accounts for the increased penetration depth resulting from the larger probe opening. Both models have rotational symmetry and the boundary conditions are identical for both models in which the bottom layer of nodes is fixed for horizontal and vertical displacements and the outer side of the tissue structure is allowed to move freely (Weickenmeier and Jabareen, 2014). In order to represent the experimental procedure which minimizes contact pressure between measurement instrument and skin surface, the contact properties between probehead and skin are modeled as a frictionless contact.

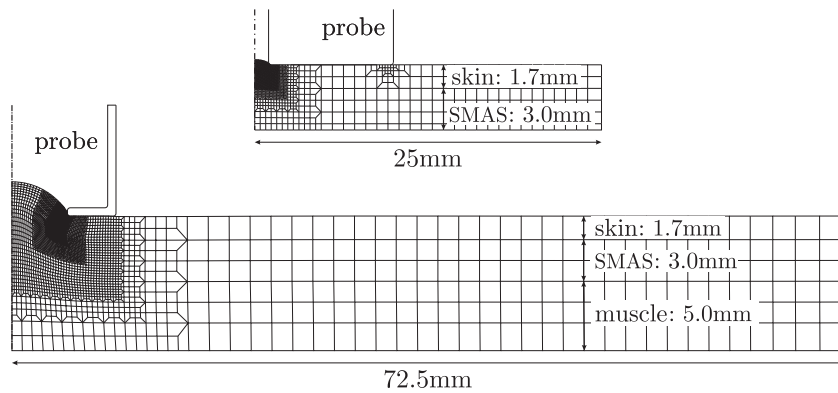


Fig. 2. FE models of the Cutometer (top) and Aspiration (bottom) device in the deformed configuration at maximum suction.

### 3.3. Parameter identification

The present optimization scheme is adapted from Weickenmeier and Jabareen (2014) and extended such to include the FE model of the Aspiration experiment. The optimization scheme minimizes the least square error between numerically predicted apex displacement and experimentally observed tissue response. Using the *fminsearch* procedure in Matlab with the Nelder–Mead simplex algorithm, two individual parameter sets for skin and SMAS were determined in parallel due to a strong influence of skin and SMAS on Cutometer and Aspiration simulations. The *fminsearch* procedure does not provide a unique solution of the optimization problem but depends on the initial values selected for the parameters. Furthermore, the procedure is affected by the coupling of the material parameters in the constitutive model. In order to ensure a robust scheme, material parameters for skin and SMAS previously determined for numerical simulations of skin wrinkling in the forehead region (Weickenmeier et al., 2014) were used as starting values. Additionally, given the strong coupling of the material model parameters, two different loading profiles for both measurement devices, therefore four different cases, must be considered to balance the individual time scales of the tissue response associated with creep and relaxation. In particular, to encompass the full range of tissue behavior observed in the experimental campaign, Cutometer measurements *instant 300 mbar* and *linear 15 mbar/s* as well as Aspiration measurements *instant 200 mbar* and *linear 15 mbar/s* were used in the optimization. This particular choice of measurements provides a broad spectrum of kinematic configurations and adds to the robustness of the optimization scheme which required more than 400 iterations to obtain an optimal set of parameters.

A schematic representation of the optimization scheme is shown in Fig. 3, where  $\mathbf{z}_0$  represents the vector of initial parameters,  $\mathbf{z}$  is the vector of the iteratively adapted parameters, *sim\_data* contains the numerically predicted apex displacements of the four loading cases, *exp\_data* provides the experimentally observed tissue response,  $f$  is the least square error, and  $\mathbf{z}_{\text{opt}}$  stores the final results of the optimization scheme. Based on Weickenmeier and Jabareen (2014), 6 of 15 material parameters per layer are included in the optimization including  $\{\mu_0, q, n, m_2, \Gamma_1, \Gamma_2, r_2\}$ .

## 4. Results

### 4.1. Experimental data

The Cutometer and Aspiration measurements are summarized in Fig. 4 in form of facial averages allowing for a comparison of the two loading cases of instant and linear loading. For the presentation of all measurements within the experimental campaign, the

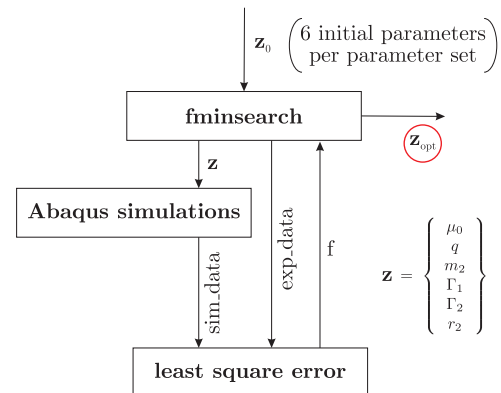


Fig. 3. Schematic representation of the optimization scheme for the material parameter identification. The Matlab function *fminsearch* minimizes the least square error of the difference between numerically predicted and experimentally observed tissue responses.

reader is referred to the supplementary documentation alongside this paper. The data was normalized with respect to the total measurement time which differs for the two devices.

The location dependent behavior is shown in Fig. 5 which visualizes the facial average together with the location specific response for the four representative measurements used in the parameter optimization. The experimental data reveals a good repeatability within the individual measurements per loading case for both devices. **In the Cutometer tests, forehead tissue showed the stiffest response, while jaw was softest.** This response is in line with anatomical data stating that skin is thickest in the forehead in comparison to parotid and jaw. The observed apex height at maximum load in repeated measurements in the same testing location varied by a maximum of 4% for instant loading and less than 10% for linear loading. Similar values were found for the Aspiration measurements where the apex height due to instant loading varied by less than 6% and by a maximum of 12% in linear loading cases. **The apex height for the averaged facial tissue response in Aspiration measurements is five times greater in comparison to the Cutometer for the difference in probehead opening diameter of factor four (Cutometer 2 mm, Aspiration device 8 mm).**

Location specific maximum apex displacements in skin were found to differ from the facial average by up to 18%, as for the case of instant loading in the jaw region (11% for the forehead and 7% for the parotid); the three regions were observed to behave very similar under linear loading: 17% higher apex displacement in the jaw in comparison to the facial average (12% lower apex displacement for the forehead and 5% for the parotid region). Location specificity in



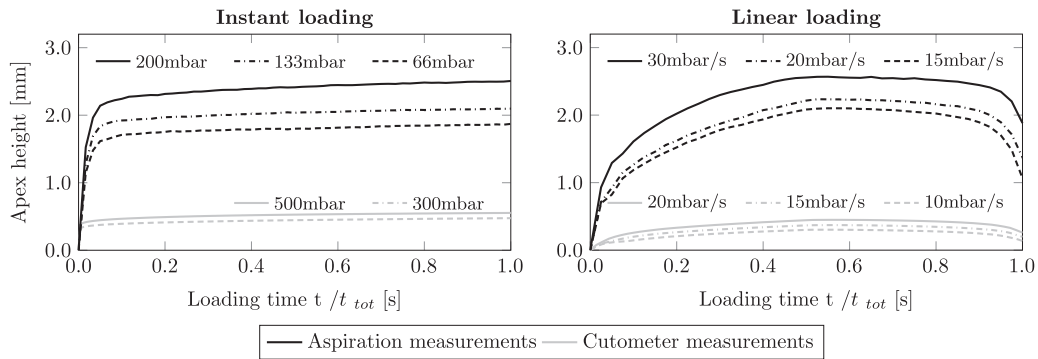


**Fig. 4.** Summary of the experimental campaign in terms of facial averages for all measurement protocols. A distinct difference in tissue response between Cutometer and Aspiration measurements is observable, as well as a very consistent and reliable increase in apex deformation for increasing loading magnitudes. Gray curves are Cutometer averages, black curves are Aspiration averages.

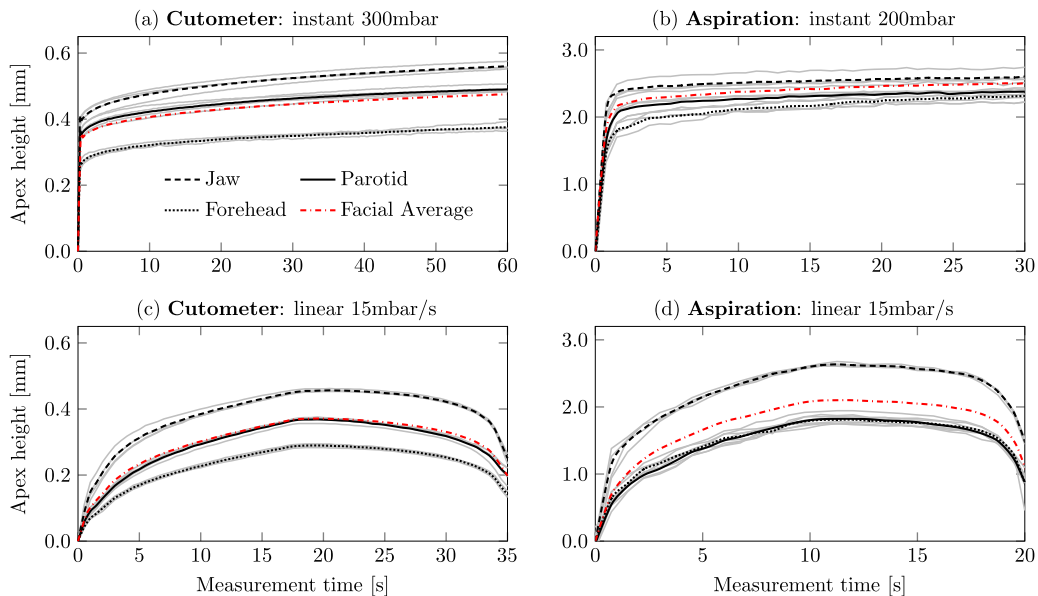


**Fig. 5.** Visualization of location dependent tissue response for four characteristic loading profiles. Gray curves represent individual measurements, black curves are the location dependent averages of these at least four measurements per site, and red lines represent the facial average curves for the respective loading profiles.

Aspiration measurements appeared to be weaker, with a maximum difference of 6% in instant loading and 14% in linear loading.

#### 4.2. Mechanical model parameters

The model parameters of the optimization are shown in Table 2. Based on the present data, they represent the most reliable set of values for the representation of average facial skin and subcutaneous tissue. Following Weickenmeier and Jabareen (2014), the parameters included in the optimization were chosen for their relevance with respect to the two different types of measurements. The initial response to suction loading is mainly determined by  $\mu_0$ ,  $q$ ,  $m_2$ , and  $\Gamma_2$ .  $\Gamma_1$  and  $r_2$  are included in order to fit the linear loading and unloading experiments at different strain rates. The parameter  $m_5$  was chosen to be  $1 - m_2$  which ensures that in the case of purely elastic deformation the shear modulus is given solely by  $\mu_0$ . The parameter  $m_3$  associated with the contribution of fibers in the tissue is set to 0, as the tissue is assumed to behave isotropically. The remaining material parameters are based on work by Rubin and Bodner (2002, 2004). In particular, the material model parameters obtained from the solution of the inverse problem resulted in a stiffer behavior of skin compared to SMAS with typical values of initial shear modulus of 2.32 kPa (skin) and 0.05 kPa (SMAS).

## 5. Discussion

### 5.1. Experimental data

Even though a direct comparison with data found in the literature is impaired by differences in measurement protocols, measurement sites, and loading magnitudes, the observed maximum apex displacements fall within values reported on forearm and cheek skin for measurements with similar probe opening diameters and instant loading profiles. The data clearly show that there is a consistent increase in apex height with increasing loading magnitude for both loading types and a similar tissue deformation behavior for both devices. Moreover, the pronounced apex height in Aspiration measurements in comparison to the Cutometer measurements clearly demonstrates the involvement of SMAS due to a larger probe opening diameter. In case of the Aspiration measurements, there is a noticeable indication for two distinct deformation patterns. While measurements in the forehead and parotid region reveal a similar response, the jaw region shows a significantly softer behavior leading to a larger apex displacement. These findings are in line with data reported by Ghassemi et al. (2003), who differentiate between two types of SMAS which appear in distinct regions of the face, the one in the jaw region being softer due to a network of relatively small fibrous septa which envelop lobules of

**Table 2**  
Model parameters for facial tissues.

	skin	SMAS	muscle
	From parameter identification		
$\mu_0$ [MPa]	0.086	0.004	0.37 <sup>a</sup>
$q$	39.74	21.58	25.0
$m_2$	0.027	0.014	0.0008
$\Gamma_1$ [Hz]	1.34	5.89	0.005
$\Gamma_2$	67.3	43.7	20.0
$r_2$	6.91	1.74	1.3
$m_1$	1000.0	1000.0	1000.0
$m_3$	0.0	0.0	0.0
$m_4$	1.0	1.0	1.0
$m_5$	0.981	0.987	0.0
$n$	0.5	1.0	1.0
$r_1$	20.0	0.2	0.2
$r_3$ [Hz]	$1.0 \cdot 10^{-10}$	$1.0 \cdot 10^{-8}$	$1.0 \cdot 10^{-8}$
$r_4$ [Hz]	$1.0 \cdot 10^{-4}$	$1.0 \cdot 10^{-4}$	$1.0 \cdot 10^{-4}$
$r_5$	1.0	1.0	1.0

<sup>a</sup>The initial shear modulus of muscle presented by Barbarino et al. (2011) was adapted to preserve the order of magnitude between skin and muscle stiffness in the presented study.

fat cells. The observed response may be explained by the particular functionality of the SMAS which has to (i) enable high flexibility for movements of the mouth in the raw regions, (ii) serve as an anchoring point of lower facial tissues in the parotid region, and (iii) allow for large deformability and strong connectivity between multiple tissue layers during wrinkle formation in the forehead region. Furthermore, deeper layers in the jaw region are generally fatty tissues and have no insertion points with any bone structure which contributes to the high level of deformability. In contrast, the deeper layers in the parotid and forehead region consist mainly of dense connective tissues which provide increased support leading to a similar response in both regions and a noticeably lower apex displacement with respect to the forehead region. In particular, the literature provides several studies on forearm skin with apex heights of 0.12–0.42 mm (Piérard et al., 2013b, probe  $\varnothing$  2 mm, pressure 500 mbar) and 1.1–1.6 mm (Hendriks et al., 2006, probe  $\varnothing$  6 mm, pressure 200 mbar). Measurements by Hara et al. (2013) indicate a stiffer behavior of skin in the region of the cheek given reported apex displacements of 0.12–0.42 mm for the same experimental configuration (probe  $\varnothing$  2 mm, pressure 500 mbar).

In contrast to these experiments, the suction device presented by Iivarinen et al. (2013) uses an elliptical probe opening in order to characterize anisotropic effects of the superficial tissue layers. The rather large probe opening ( $43 \times 28$  mm) leads to apex displacements ranging from 1.20 to 2.25 mm for suction pressures of 200 mbar on forearm tissue. However, the comparatively large probe opening may also lead to an increased homogenization of the mechanical response across multiple tissue layers including a compromised representation of their anisotropic behavior.

## 5.2. Comparison of material parameters

In the literature, the experimental data from suction experiments is most often used for the determination of Young's modulus or the initial shear modulus. Although testing methods, constitutive model formulations, and measurement sites considered in the determination of initial shear moduli of distinct tissues may differ significantly, the shear values presented in this work fall well within the range of reported data. Initial shear values  $\mu_0$  for skin range from 0.5 kPa (Bader and Bowker, 1983) to 19 kPa (Hendriks et al., 2003) while the initial shear modulus, given by  $\tilde{\mu}_0 = \mu_0 \cdot m_2$ , was found to be 2.32 kPa. Similarly, values for SMAS (or the location dependent equivalent) range from 0.04 kPa (Hendriks et al., 2003) to 8.7 kPa (Weaver, 2005) with the determined value of 0.05 kPa falling within the limits reported in the literature.

The direct comparison of the present work with data presented by Rubin and Bodner (2002) reveals a significant discrepancy of the initial shear moduli (27 kPa for skin and 15 kPa for SMAS) despite using the same material model. This pronounced deviation may be explained by the experimental characterization of both skin and SMAS based on ex vivo uniaxial tension tests of excised tissue samples, which may lead to an overestimation of tissue stiffness. The difference between our initial shear moduli and the values presented by Barbarino et al. (2011) (skin: 8.24 kPa and SMAS: 1.29 kPa) is most certainly related to the incorporation of the dissipative tissue response in our study in comparison to the implementation of the purely elastic part by Barbarino et al. (2011). Finally, the differences of skin parameters with respect to our previous work by Weickenmeier and Jabareen (2014) result from the involvement of deeper tissue layers.

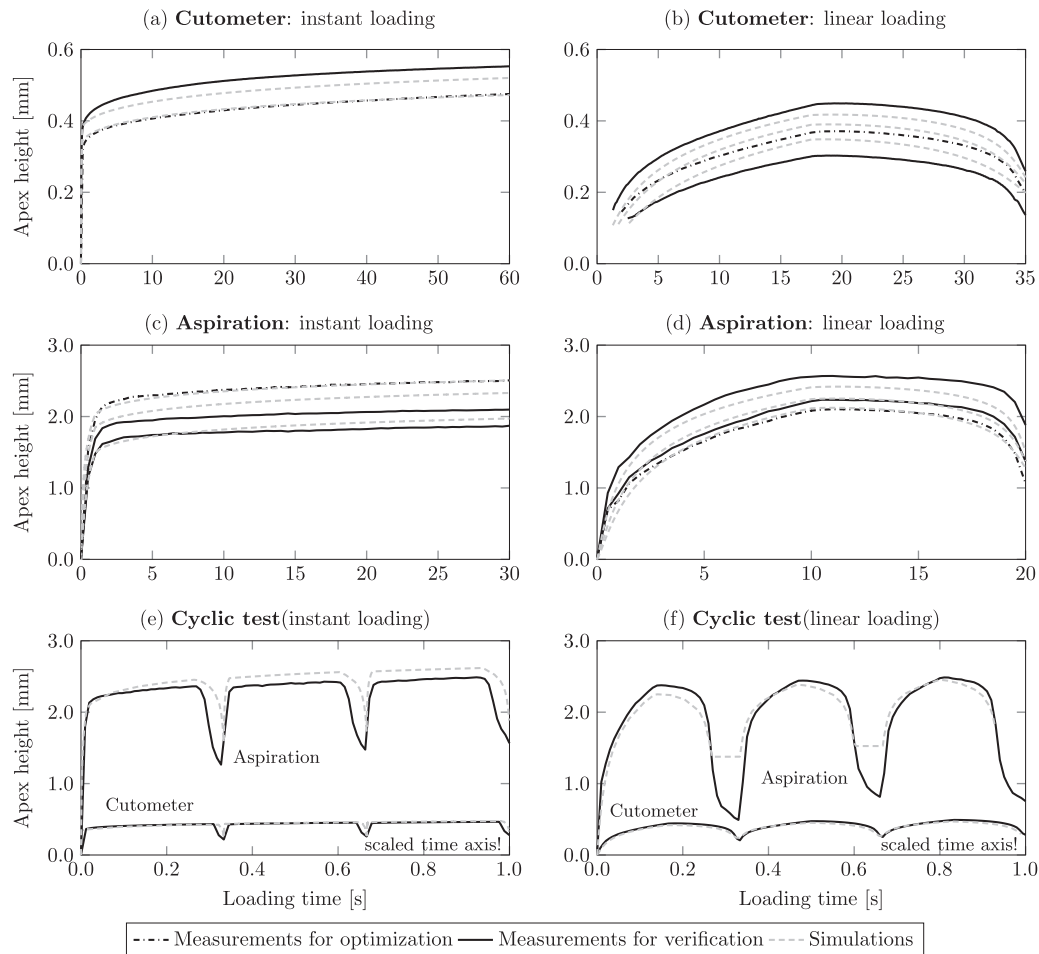


**Fig. 6.** Comparison of experimental data and numerical simulation based on the newly proposed material parameters. The cyclic data is shown on a scaled time axis due to differences in the Aspiration and Cutometer measurement protocols (31 s and 60 s loading time per cycle, respectively).

### 5.3. Comparison of experimental and numerical results

The direct comparison of experimental and numerical curves, as shown in Fig. 6, reveals a good agreement for nearly all loading cases presented within this study, thus, demonstrating the reliability of the measurement data as well as the good predictive capabilities of the constitutive model equations. The concise representation of the cyclic data highlights the model's capability to capture the history dependent response of skin and SMAS. The maximum absolute error between predicted and measured apex height at  $t_{\text{fin}}$  is less than 10%.

### 5.4. Sensitivity analysis

The impact of the proposed boundary conditions and variations in material parameters needs verification for both FE models. While the Cutometer model was previously investigated (Weickenmeier and Jabareen, 2014), the sensitivity of the Aspiration model was analyzed here. Two different loading cases were considered (instant 200 mbar, linear 15 mbar/s) while initial shear modulus of muscle ( $C_1$ – $C_3$ ), the boundary conditions of the nodes at the bottom of the muscle layer ( $C_4$  and  $C_5$ ), and the contact properties between the skin surface layer and the suction probe ( $C_6$ ) were varied. These simulations are compared to the numerical results of the optimization scheme which are considered as the reference cases. As shown in Fig. 7, the impact of muscle stiffness may be considered marginal as the relative error of maximum apex height between the reference setting and the individual

simulations is less than 1.3%, independent of instant or linear loading. The two most influential settings  $C_4$  (no displacement constraints on the bottom nodes of muscle) and  $C_6$  (tight contact between skin and probe) result in a relative error of maximally 3.3% and 6.2%, respectively. Despite an increased sensitivity, however, these two cases contrast the experimentally observed sliding between skin and probehead during measurements as well as the anatomical property of muscle innervating deeper tissues and bone, especially in the regions of interest to our study.

The proposed optimization scheme determines material parameters for skin and SMAS simultaneously, since a strong dependence of both FE models on the skin layer was observed. Table 3 shows the results of a sensitivity analysis that demonstrates this coupling of both FE models using the example of varying two characteristic material parameters, i.e. the initial shear modulus  $\mu_0$  and the constant controlling the nonlinearity of the strain energy function  $q$ , of skin and SMAS. From this data it is concluded that (i) both models show a clear dependence on the parameters of skin, since the relative error in the Aspiration and Cutometer model are in the same order of magnitude and (ii) the variation of SMAS primarily affects the predicted apex height of the Aspiration model while the Cutometer model is nearly unaffected. In particular, the latter observation is in line with the previous analysis of the Cutometer model (Weickenmeier and Jabareen, 2014). Due to this similar dependence of the Cutometer and Aspiration model on the properties of skin tissue, a sequential optimization of skin parameters using Cutometer data only and the subsequent determination of SMAS parameters using only Aspiration data is not feasible.

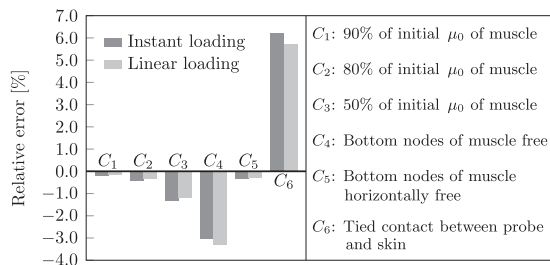


Fig. 7. Sensitivity analysis on the FE model of the Aspiration measurement.

Table 3

Relative error of maximum apex height calculated from the optimization scheme and numerical simulations with varied material parameters  $\mu_0$  and  $q$ . Relative errors indicate the strong coupling between skin and SMAS in the Cutometer and Aspiration FE model.

Parameter	Aspiration		Cutometer	
	Instant 200 mbar (%)	Linear 15 mbar/s (%)	Instant 300 mbar (%)	Linear 15 mbar/s (%)
80% $\mu_0$ skin	-1.4	-2.3	-4.6	-5.6
80% $q$ skin	-2.3	-2.9	-7.5	-7.3
80% $\mu_0$ SMAS	-1.3	-1.6	-0.04	-0.05
80% $q$ SMAS	6.1	5.9	0.002	0.07

## 6. Conclusion

The numerical simulation of facial soft tissues is gaining importance for the medical community as it will allow us to improve predictions of the tissue response in facial expressions, aging, and surgical interventions. The experimental characterization and numerical simulation of facial soft tissue structures play a key role in advancing our current understanding of their mechanical response. The presented experimental campaign provides Cutometer and Aspiration data on the location, time, and loading history dependent mechanical properties of facial skin and SMAS. Moreover, the proposed optimization scheme allowed us to determine two sets of parameters for the Rubin and Bodner material model. The presented material parameters for skin and SMAS show very good agreement between the experimentally observed and numerically predicted tissue response, including the history dependent tissue behavior.

In order to improve the agreement between experimental suction data and numerically predicted tissue behavior, future work should incorporate the anisotropic nature of skin and deeper tissue layers as well as the in vivo pre-stress state of superficial skin layers. These changes require the extension of the finite element models to three-dimensional representations and an experimental method to quantify the anisotropic contribution to the overall tissue response. To this end, suction experiments using devices with an elliptical (instead of circular) opening might be considered. The influence of friction needs being considered in greater detail through specific measurements providing a range of realistic values of the friction coefficient between probehead and skin. Moreover, the presented material parameters were shown to closely represent the multi-axial loading state of suction experiments, while the performance under homogeneous loading cases, e.g. uniaxial or biaxial tension, needs to be investigated. And finally, the developed experimental setup may be used for intra- and inter-subject comparison; it will be applied in future studies considering a large group of subjects with different types of skin, especially targeting subgroups with aged and diseased tissues. Measurements will not only provide age, subject, and location specific material parameters but also help identifying response patterns associated with pathological skin behavior.

## Conflict of Interest

There is no conflict of interest.

## Appendix A. Supplementary data

Supplementary data associated with this article can be found in the online version at <http://dx.doi.org/10.1016/j.jbiomech.2015.10.039>.

## References

- Abellan, M.A., Zahouani, H., Bergheau, J., 2013. Contribution to the determination of in vivo mechanical characteristics of human skin by indentation test. *Comput. Math. Methods Med.*, 11 p.
- Bader, D., Bowker, P., 1983. Mechanical characteristics of skin and underlying tissues in vivo. *Biomaterials* 4, 305–308.
- Barbarino, G., Jabareen, M., Mazza, E., 2011. Experimental and numerical study on the mechanical behaviour of the superficial layers of the face. *Skin Res. Technol.* 17, 434–444.
- Bhushan, B., Tang, W., Ge, S., 2010. Nanomechanical characterization of skin and skin cream. *J. Microsc.* 240, 135–144.
- Bischoff, J., Arruda, E., Grosh, K., 2004. A rheological network model for the continuum anisotropic and viscoelastic behavior of soft tissue. *Biomech. Model. Mechanobiol.* 3, 56–65.
- Courage and Khazaka, 2014. *Electronic GmbH*. Köln, DE.
- Flynn, C., Taberner, A., Nielsen, P., 2011. Mechanical characterisation of in vivo human skin using a 3D force-sensitive micro-robot and finite element analysis. *Biomech. Model. Mechanobiol.* 10, 27–38.
- Fung, Y., 1993. *Biomechanics: Mechanical Properties of Living Tissues*. Springer, New York.
- Ghassemi, A., Prescher, A., Riediger, D., Axer, H., 2003. Anatomy of the smas revisited. *Aesthet. Plast. Surg.* 27, 258–264.
- Hara, Y., Masuda, Y., Hirao, T., Yoshikawa, N., 2013. The relationship between the Young's modulus of the stratum corneum and age: a pilot study. *Skin Res. Technol.* 19, 339–345.
- Hendriks, F., Brokken, D., Oomens, C., Bader, D., Baaijens, F., 2006. The relative contributions of different skin layers to the mechanical behavior of human skin in vivo using suction experiments. *Med. Eng. Phys.* 28, 259–266.
- Hendriks, F., Brokken, D., Van Eemeren, J., Oomens, C., Baaijens, F., Horsten, J., 2003. A numerical-experimental method to characterize the non-linear mechanical behaviour of human skin. *Skin Res. Technol.* 9, 274–283.
- Hollenstein, M., Bugnard, G., Joos, R., Kropf, S., Villiger, P., Mazza, E., 2013. Towards laparoscopic tissue aspiration. *Med. Image Anal.* 17, 1037–1045.
- Iivarinen, J., Korhonen, R., Julkunen, P., Jurvelin, J., 2013. Experimental and computational analysis of soft tissue mechanical response under negative pressure in forearm. *Skin Res. Technol.* 19, 356–365.
- Iivarinen, J., Korhonen, R., Jurvelin, J., 2014. Experimental and numerical analysis of soft tissue stiffness measurement using manual indentation device: significance of indentation geometry and soft tissue thickness. *Skin Res. Technol.* 20, 347–354.
- Jor, J., Nash, M., Nielsen, P., Hunter, P., 2011. Estimating material parameters of a structurally based constitutive relation for skin mechanics. *Biomech. Model. Mechanobiol.* 10, 767–778.
- Kauer, M., Vuskovic, V., Dual, J., Székely, G., Bajka, M., 2002. Inverse finite element characterization of soft tissues. *Med. Image Anal.* 6, 275–287.
- Nava, A., Mazza, E., Kleiner, F., Avis, N., McClure, J., Bajka, M., 2004. Evaluation of the mechanical properties of human liver and kidney through aspiration experiments. *Technol. Health Care* 12, 269–280.
- Piérard, G., Hermans-Lê, T., Piérard-Franchimont, C., 2013a. Scleroderma: skin stiffness assessment using the stress-strain relationship under progressive suction. *Expert Opin. Med. Diagn.* 7, 119–125.
- Piérard, G., Piérard, S., Delvenne, P., Piérard-Franchimont, C., 2013b. In vivo evaluation of the skin tensile strength by the suction method: pilot study coping with hysteresis and creep extension. *ISRN Dermatol.*, 7, pages.
- Rubin, M., Bodner, S., 2002. A three-dimensional nonlinear model for dissipative response of soft tissue. *Int. J. Solids Struct.* 39, 5081–5099.
- Rubin, M., Bodner, S., 2004. Modeling nonlinear dissipative response of biological tissues. *Int. J. Solids Struct.* 41, 1739–1740.
- Tarsi, G., Gould, R., Chung, J., Xu, A., Bozkurt, A., Butcher, J., 2013. Method for non-optical quantification of in situ local soft tissue biomechanics. *J. Biomech.* 46, 1938–1942.
- Weaver, J.B., Doyley, M., Cheung, Y., Kennedy, F., Madsen, E.L., Van Houten, E.E., Paulsen, K., 2005. Imaging the shear modulus of the heel fat pads. *Clin. Biomech.* 20, 312–319.
- Weickenmeier, J., Jabareen, M., 2014. Elastic-viscoplastic modeling of soft biological tissues using a mixed finite element formulation based on the relative deformation gradient. *Int. J. Numer. Methods Biomed. Eng.* 30, 1238–1262.
- Weickenmeier, J., Wu, R., Lecomte-Grosbras, P., Witz, J.-F., Brieu, M., Winkhofer, S., Andreisek, G., Mazza, E., 2014. Experimental characterization and simulation of layer interaction in facial soft tissues. *Lect. Notes Comput. Sci.* 8789, 233–241.